Journal of Inorganic and General Chemistry
ZAAC
Zeitschrift für anorganische und allgemeine Chemie
DOI: 10.1002/zaac.201700046
ARTICLE

$Li_4Ba[BN_2]_2$ – Structure and Vibrational Spectra

Stefan Seidel,[a] Mehmet Somer,[b] Kamil Kiraz,[b] Ute Ch. Rodewald,[a] and Rainer Pöttgen*[a]

Dedicated to Professor Thomas Schleid on the Occasion of his 60th Birthday

Abstract. The nitridoborate $Li_4Ba[BN_2]_2$ was synthesized from a 4:1 molar ratio of $Li_3[BN]_2$ and $Ba_3[BN_2]_2$ in an arc-welded niobium ampoule at a maximum annealing temperature of 1173 K. The structure was refined from single-crystal X-ray diffractometer data: new type, $P\bar{1}$, a = 533.9(2), b = 585.0(3), c = 860.6(4) pm, α = 80.72(3), β = 73.84(6), γ = 89.87(4)°, wR_2 = 0.1196, 1429 F^2 values, 50 variables. The $Li_4Ba[BN_2]_2$ structure contains two crystallographically independent $[BN_2]^{3-}$ units with 134 pm B–N distance, which are slightly bent: 178° for N2–B1–N1 and 175° for N4–B2–N3. Due to the high lithium content both $[BN_2]^{3-}$ units have a strongly distorted coordination by $8Li^+ + 3Ba^{2+}$. The four crystallographically independent lithium cations show distorted tetrahedral coordination by $[BN_2]^{3-}$ units with Li–N distances ranging from 195 to 247 pm. IR and Raman spectra show the typical vibrations of the $[BN_2]$ unit along with a well-resolved splitting of the $\nu(^{10}B)$ and $\nu(^{11}B)$ frequencies.

Introduction

The linear nitridoborate anion $[BN_2]^{3-}$ is isoelectronic with carbon dioxide and it is one of the basic building units in diverse nitridoborates.[1] Such phases form with the alkali metals lithium (α- and β-$Li_3[BN_2]$)[2–5] and sodium ($Na_3[BN_2]$ and an ordered phase $Na_2K[BN_2]$)[6,7] and the alkaline earth metals.[8–12] In the latter case, polymorphism has been observed for the calcium and strontium compound and $Ba_3[BN_2]_2$[9] shows a distinctly different arrangement of the $[BN_2]^{3-}$ units. Combing an alkali and an alkaline earth cation leads to ordered phases, e.g. $LiMg[BN_2]$,[13] $LiCa_4[BN_2]_3$,[14] or $SrBa_8[BN_2]_6$.[15]

Ordered nitridoborate structures are also known for two different anions. Typical examples are the nitridoborate nitride $Ca_3[BN_2]N$[16] or the nitridoborate oxide $Ba_4[BN_2]_2O$.[17] The largest number of such compounds exists for nitridoborate halides,[18] e.g. $M_2[BN_2]X$ (M = Ca, Sr, Eu; X = F, Cl, Br, I),[19–21] $Ca_3[BN_2]I_3$,[22] or $Ba_8[BN_2]_5F$.[23] The nitridoborate hydride $Ca_2[BN_2]H$[24] is isotypic with the fluoride $Ca_2[BN_2]F$.[19] An overview on the different alkali and alkaline earth cation coordination modes of the $[BN_2]^{3-}$ anion is compiled in Figure 1. The coordination number depends on the size and electronegativity of the counter elements.

The vibrational spectroscopic behavior of the linear or slightly bent $[BN_2]^{3-}$ units has been studied in detail for most of the nitridoborates by IR and Raman spectroscopy.[26] Those nitridoborates containing divalent europium show interesting magnetic properties. $Eu_3[BN_2]_2$ and $LiEu_4[BN_2]_3$ show ferromagnetic ordering at T_N = 32 and 22 K, respectively.[10] Slightly lower magnetic ordering temperatures (possibly antiferromagnetic ordering) of 9.7, respectively 7.3 K have been reported for $Eu_2[BN_2]Br$ and $Eu_2[BN_2]I$.[20] Most recent studies concern the luminescence properties of undoped and Eu^{2+} doped nitridoborates mainly with respect to red emission.[27–29]

During recent crystallization experiments for $LiBa_4[BN_2]_3$[30] we obtained well-shaped single crystals of the

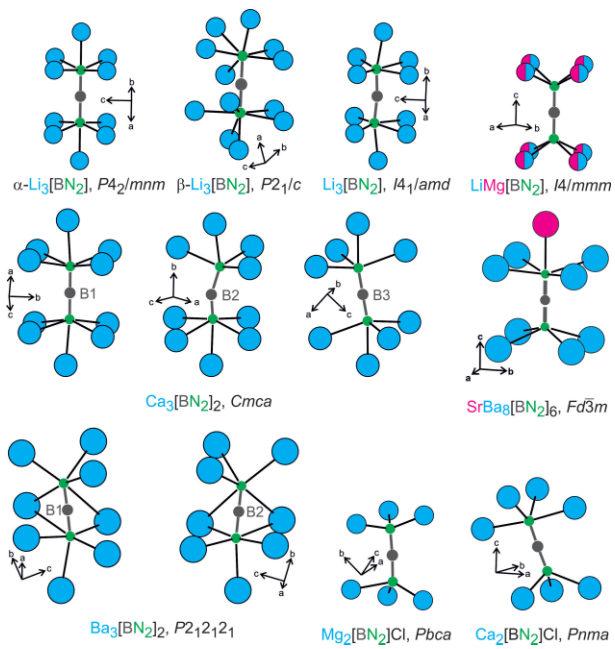


Figure 1. Coordination of $[BN_2]^{3-}$ units in diverse alkali and alkaline earth metal nitridoborates. Crystallographic data were taken from the Pearson data base.[25]

* Prof. Dr. R. Pöttgen
Fax: +49-251-83-36002
E-Mail: pottgen@uni-muenster.de
[a] Institut für Anorganische und Analytische Chemie
Universität Münster
Corrensstrasse 30
48149 Münster, Germany
[b] Chemistry Department
Koc University
Rumelifeneri Yolu
34450 Sariyer-Istanbul, Turkey

 © 2017 WILEY-VCH Verlag GmbH & Co. KGaA, Weinheim

lithium-rich nitrodoborate $Li_4Ba[BN_2]_2$. The targeted synthesis, crystal chemical details, and the spectroscopic behavior of the new structure type are reported herein.

Experimental Section

Synthesis: $Li_4Ba[BN_2]_2$ was accidently discovered during the attempts to synthesize $LiBa_4[BN_2]_3$, which is the missing link in the series $LiM_4[BN_2]_3$ (M = Ca, Sr, Eu^{II}). In a targeted synthesis, the title compound was accessible via a high-temperature reaction of $Li_3[BN]_2$[2] and $Ba_3[BN_2]_2$[9] in the molar ratio of 4:1 in an arc-welded niobium ampoule, which in turn was encapsulated in an evacuated and sealed silica tube to avoid oxidation (typical batch: 0.75–1.5 g). The sample was heated to 1173 K during 4 h, annealed for 10 h and finally cooled down to room temperature within 24 h. The final product consists of transparent white to gray crystallites, which decompose readily under release of NH_3 gas when exposed to air and moisture. Therefore, all sample handling and preparations were performed in an argon box ($H_2O \leq 1$ ppm and $O_2 \leq 1$ ppm).

X-ray Image Plate Data and Data Collection: The polycrystalline $Li_4Ba[BN_2]_2$ sample was characterized by X-ray powder diffraction with a Bruker D2 Phaser powder diffractometer with Cu-K_α radiation in the 2θ range of 10–90° at a step size of 0.02°and at a rate of 0.3°·min^{-1}. The triclinic lattice parameters (see Table 1) were obtained from least-squares fit to the powder data. Correct assignment of the diffraction intensities was ensured by comparison with a calculated pattern using the LAZYPULVERIX routine.[31]

Table 1. Crystallographic data and structure refinement for $Li_4Ba[BN_2]_2$.

	$Li_4Ba[BN_2]_2$
Molar mass /g·mol^{-1}	242.8
Space group	$P\bar{1}$
Lattice parameters, (powder data)	
a /pm	533.9(2)
b /pm	585.0(3)
c /pm	860.6(4)
α /°	80.72(3)
β /°	73.89(4)
γ /°	89.87(4)
Cell volume /nm^3	0.2546
Density calcd. /g·cm^{-3}	3.17
Z	2
Crystal size /µm	$10 \times 15 \times 20$
Detector distance /mm	40
Exposure time /s	180
ω range; step width /°	0–180; 0.3
Integr. parameters, A; B; EMS	7.0; –6.0; 0.030
$h\ k\ l$ range	±7, ±8, ±12
θ range for data collection, deg	2.5–32.1
Transm. ratio, max /min	0.589 / 0.463
Linear absorption coeff. /mm^{-1}	7.7
No. of reflections	2937
Independent reflections / R_{int}	1429 / 0.0627
Reflections with $I \geq 2\sigma(I)$ / R_σ	731 / 0.1576
$F(000)$, e	212
R_1 / wR_2 for $I \geq 2\sigma(I)$	0.0504 / 0.0889
R_1 / wR_2 for all data	0.1178 / 0.1196
Data / parameters	1429 / 50
Goodness-of-fit on F^2	0.99
Largest diff. peak /hole /e·Å^{-3}	1.63 / –1.88

Irregularly shaped single crystal fragments were separated from the mechanically fragmented sample of the initial composition $LiBa_4[BN_2]_3$. The crystals were glued to quartz fibers with beeswax and were kept in Schlenk tubes in a dry argon atmosphere to protect for hydrolyses. The crystal quality was first checked by Laue photographs on a Burger camera (white molybdenum radiation, image plate technique, Fujifilm, BAS-1800). Intensity data of a suitable single crystal was collected with a Stoe StadiVari single crystal diffractometer equipped with a Mo micro focus source and a Pilatus detection system. The Gaussian-shaped profile of the X-ray source required scaling along with numerical absorption corrections. All relevant crystallographic data and details of the data collection and evaluation are listed in Table 1.

Further details of the crystal structure investigations may be obtained from the Fachinformationszentrum Karlsruhe, 76344 Eggenstein-Leopoldshafen, Germany (Fax: +49-7247-808-666; E-Mail: crysdata@fiz-karlsruhe.de, http://www.fiz-karlsruhe.de/request for deposited data.html) on quoting the depository number CSD-432641.

Vibrational Spectroscopy: FT-Raman spectra were recorded with a Raman microscope RENISHAW inVia with a 532-nm excitation laser source. For the measurement of the air-sensitive sample, the material was filled in the argon box into a Pyrex tube (Ø = 4 mm) and later sealed using a propane torch. The IR spectra were registered with a Thermo Scientific iS50 equipped with a reflection ATR module.

Results and Discussion

Structure Refinement

Careful analyses of the diffractometer data set revealed a triclinic lattice. The centrosymmetric space group $P\bar{1}$ was found to be correct during the structure refinement. The starting atomic parameters were obtained with the charge-flipping algorithm of Superflip.[32] The structure was subsequently refined on F^2 with anisotropic displacement parameters for the barium atoms [U_{11} = 229(3), U_{22} = 243(3), U_{33} = 281(4), U_{12} = 4(2), U_{13} = –18(3), U_{23} = –51(3) pm^2] and isotropic ones for the light atoms using the Jana2006[33] routine. The final difference Fourier synthesis was flat. The refined positional parameters, displacement parameters, and interatomic distances are listed in Table 2 and Table 3.

Table 2. Atomic coordinates and equivalent isotropic displacement parameters /pm^2 for $Li_4Ba[BN_2]_2$. All atoms lie on Wyckoff sites 2*i*. U_{eq} is defined as one third of the trace of the orthogonalized U_{ij} tensor.

Atom	x	y	z	U_{eq}
Li1	0.041(4)	0.166(4)	0.383(3)	270(50)
Li2	0.556(4)	0.175(3)	0.391(3)	210(40)
Li3	0.826(5)	0.433(4)	0.136(3)	280(50)
Li4	0.831(5)	0.013(4)	0.136(3)	350(60)
Ba	0.3392(2)	0.68691(17)	0.25125(13)	261(2)
B1	0.303(3)	0.225(2)	0.0938(16)	180(20)
B2	0.205(3)	0.340(2)	0.6046(17)	220(30)
N1	0.139(2)	0.2474(17)	0.0005(13)	240(20)
N2	0.476(2)	0.2043(17)	0.1816(13)	240(20)
N3	0.186(2)	0.5637(18)	0.6227(14)	270(20)
N4	0.2034(19)	0.1138(16)	0.5966(12)	195(19)

© 2017 WILEY-VCH Verlag GmbH & Co. KGaA, Weinheim

Table 3. Selected interatomic distances /pm in the structure of $Li_4Ba[BN_2]_2$. Standard deviations are given in parentheses.

Li1:	N3	199(3)	B2:	N4	134(2)
	N4	205(2)		N3	134(2)
	N4	222(3)		Li2	254(2)
	N2	247(2)		Li1	265(3)
Li2:	N2	195(3)		Li3	274(3)
	N3	203(2)		Li4	275(3)
	N4	213(2)		Ba	282(1)
	N4	218(2)		Ba	302(2)
Li3:	N1	202(2)	N1:	B1	134(2)
	N3	206(3)		Li3	202(2)
	N1	216(3)		Li4	205(3)
	N2	221(3)		Li4	209(2)
Li4:	N1	205(3)		Li3	216(3)
	N1	209(2)		Ba	299.8(9)
	N2	217(3)		Li1	314(3)
	N4	226(3)	N2:	B1	134(2)
Ba:	B2	282(1)		Li2	195(3)
	N1	299.8(9)		Li4	217(3)
	N3	300(1)		Li3	221(3)
	B1	302(1)		Li1	247(2)
	B2	302(2)		Ba	303(1)
	N2	303(1)		Ba	304(1)
	N3	304(1)	N3:	B2	134(2)
	N2	304(1)		Li1	199(3)
	N4	314(1)		Li2	203(2)
B1:	N1	134(2)		Li3	206(3)
	N2	134(2)		Ba	300(1)
	Li1	246(2)		Ba	304(1)
	Li4	272(3)	N4:	B2	134(2)
	Li3	278(3)		Li1	205(2)
	Li3	280(3)		Li2	213(2)
	Li4	284(3)		Li2	218(2)
	Ba	302(1)		Li1	222(3)
				Li4	226(3)
				Ba	314(1)

Crystal Chemistry

The lithium-rich nitridoborate $Li_4Ba[BN_2]_2$ crystallizes with a new triclinic structure type, space group $P\bar{1}$, Pearson symbol *aP*22 and Wyckoff sequence i^{11}. The structure contains two crystallographically independent $[BN_2]^{3-}$ anions, both with B–N distances of 134 pm. Both units are slightly bent with N4–B2–N3 and N2–B1–N1 angles of 175 and 178°, respectively. The two nitridoborate units are separated and charge-balanced by four lithium cations and one barium cation.

The coordination of the $[BN_2]^{3-}$ anions is presented in Figure 2, right-hand part in a ball-and-stick presentation. Although the polyhedra are both formed by eight lithium and three barium cations, they are distinctly different. Both $[BN_2]^{3-}$ anions show a new kind of mixed metal coordination in the family of nitridoborates.[34]

We start with the N1–B1–N2 unit, where the N1 and N2 atoms both have four lithium atoms in their coordination (202–216 pm N1–Li and 195–247 pm N2–Li), however, with a low-symmetric arrangement for N2, a direct consequence of the barium coordination. One of the barium atoms coordinates to the whole $[BN_2]$ unit, although with a closer Ba–N1 contact of 300 pm as compared to Ba–N2 of 353 pm. The two other barium cations do only coordinate to N1, thus explaining the longer N2–Li1 contact of 247 pm. Even though the coordination polyhedron is irregular, the $[BN_2]$ unit is almost linear with an N1–B1–N2 angle of 178°.

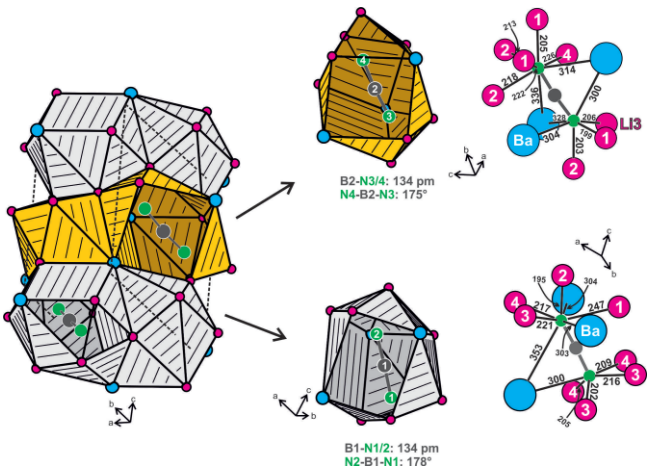


Figure 2. The crystal structure of $Li_4Ba[BN_2]_2$. Lithium, barium, boron, and nitrogen atoms are drawn as magenta, blue, medium grey, and green circles, respectively. (left) View of the unit cell with a condensation of the two independent polyhedra around the $[BN_2]$ units. (middle) Coordination polyhedra of the $[BN_2]$ units; the B–N distances and N–B–N angles are given. (right) Ball and stick representation of the lithium / barium coordination of the $[BN_2]$ units. Relevant distances are given.

The lithium coordination of the N4–B2–N3 unit (Figure 2) is asymmetric with five neighboring lithium atoms to N4 (205–226 pm N4–Li) and three neighboring lithium atoms to N3 (199–206 pm N3–Li). Two of the barium cations coordinate to the complete $[BN_2]$ unit, while the third one has only a closer contact to N3 which has the smaller number of neighboring lithium atoms.

The coordination polyhedra of both $[BN_2]$ units are shown in the middle part of Figure 2 with light grey and yellow shading. These two polyhedra are the basic building units and the $Li_4Ba[BN_2]_2$ structure forms through condensation of the polyhedra via common faces. The two crystallographically independent $[BN_2]$ units are aligned almost perpendicular to each other (see the projection approximately along *a* in Figure 3).

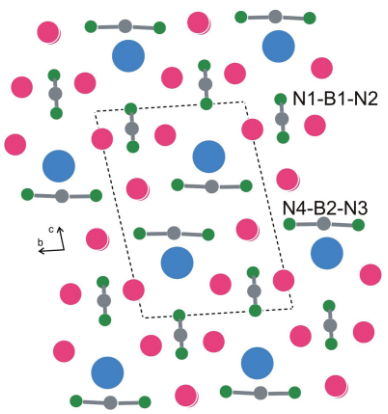


Figure 3. Arrangement of the $[BN_2]$ units in $Li_4Ba[BN_2]_2$. Lithium, barium, boron, and nitrogen atoms are drawn as magenta, blue, medium grey and green circles, respectively.

© 2017 WILEY-VCH Verlag GmbH & Co. KGaA, Weinheim

Table 4. Charge distribution analysis of $Li_4Ba[BN_2]_2$ by bond valence sums (BVS) and the CHARDI algorithm.[a)]

	Li1	Li2	Li3	Li4	Ba	B1	B2	N1	N2	N3	N4
ΣQ (BVS)[37]	0.95	1.18	1.05	0.97	1.55	2.84	2.84	–2.82	–2.84	–2.98	–2.82
ΣQ (CHARDI)[39]	0.87	1.15	1.02	0.96	1.99	3.06	2.95	–2.99	–2.94	–3.03	–3.05

a) $BV = e^{(r_0-r)/b}$. b = 0.37, r_0 (Li^I–N) = 161, r_0 (Ba^{II}–N) = 247 pm and r_0 (B^{III}–N) = 147 pm[40].

The four crystallographically independent lithium cations are all tetrahedrally coordinated by four $[BN_2]^{3-}$ units (Figure 4). The complex arrangement of the ligand units leads to substantial distortions. The Li–N distances cover a larger range from 195 to 247 pm. At least the longer Li1–N2 contact at 247 pm is only weakly bonding. Similar coordination occurs for the lithium atoms in monoclinic $Li_3[BN_2]$ with a comparable range of Li–N distances of 198–251 pm.[3] A much smaller range of Li–N distances for tetrahedral coordination occurs for the lithium atoms in the dicyanamides $LiLa(CN_2)_2$ (209–211 pm)[35] and $Li_2[CN_2]$ (207 pm).[36]

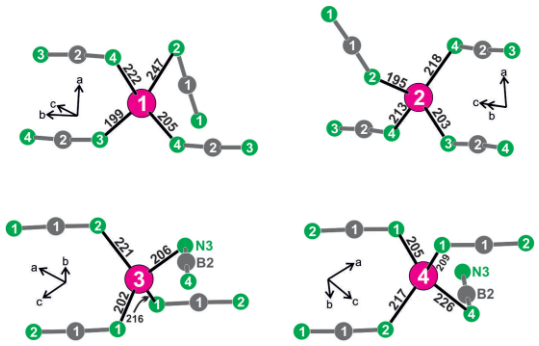


Figure 4. Coordination of the lithium atoms in the crystal structure of $Li_4Ba[BN_2]_2$. Lithium, boron, and nitrogen atoms are drawn as magenta, medium grey and green circles, respectively. Atom designations and relevant interatomic distances are indicated.

$Li_4Ba[BN_2]_2$ was further analyzed by calculations of the bond valence sums (BVS)[37] and the CHARDI algorithm.[38,39] The calculated numerical values are listed atom-by-atom in Table 4. The BVS data result from empirical parameters,[40,41] whereas CHARDI uses a point-charge approach. The ideal charges are almost well reproduced by both models. Solely the Li2 atoms show weak over-bonding in both calculations. This is in line with the shorter Li2–N distances.

Spectroscopic Characterization

The dinitridoborate groups $[N=B=N]^{3-}$ are the vibrational spectroscopically relevant moieties in $Li_4Ba[BN_2]_2$. The perfectly symmetrical anion (linear and with equal B–N distances) belongs to the point symmetry $D_{\infty h}$, for which the following three fundamentals are expected: $\Gamma_{vib}(D_{\infty h}) = \Sigma_g(\nu_1,R) + \Sigma_u(\nu_2, IR) + \Pi_u(\nu_3, IR)$.

Modes with the parity "g" are only Raman- those with "u" are only IR-active (mutual exclusion). The triclinic unit cell contains two formula units comprising 2×2 crystallographically independent $[BN_2]^{3-}$ groups, which are symmetric [d(B–N) = 134 pm] but slightly non-linear (178 and 175°). In this case a symmetry reduction from $D_{\infty h}$ (idealized) to C_{2v} (site symmetry) will occur, accompanied by splitting of the doubly degenerate mode ν_3 in two bands and the abolishment of mutual exclusion, hence, all three modes become active both in IR and Raman spectroscopy. However, the difference in the arrangement of the two distinct units and the deviation from linearity is only marginal. Thus, the vibrational spectra of $Li_4Ba[BN_2]_2$ can be interpreted under the assumption of crystallographically equivalent $[N=B=N]^{3-}$ groups with $D_{\infty h}$ symmetry, taking the isotope splitting of the $^{11}B/^{10}B$ pairs with the band intensity ratio of $I(^{11}B)/I(^{10}B)$ = 4:1 (in accordance with the natural abundance 80/20 of two boron isotopes) and $\nu(^{10}B)/\nu(^{11}B) \approx 0.95$ into account.

In the vibrational spectra (Figure 5), the characteristic symmetric (B–N) stretch ν_1 is observed as a very intense Raman band at 1050 cm^{-1}. The IR pendant is located at 1062 cm^{-1}. The antisymmetric (B–N) valence vibration $\nu_2(^{11}B)$ appears as a very strong IR absorption at 1685 cm^{-1}. Due to the isotope effect, the corresponding $\nu_2(^{10}B)$ is slightly blue shifted and is observed at 1756 cm^{-1}. In accordance with the predictions, the in-plane deformation $\nu_3(^{11}B)$ splits up into two modes ν_{3a} = 599 and ν_{3b} = 622 cm^{-1}. The weak satellite at 644 cm^{-1} is assigned to its ^{10}B component. The weak IR band at 790 cm^{-1} is definitely not a fundamental and can be interpreted either as a lattice vibration, in which predominantly the light Li atoms are involved or a combination mode.

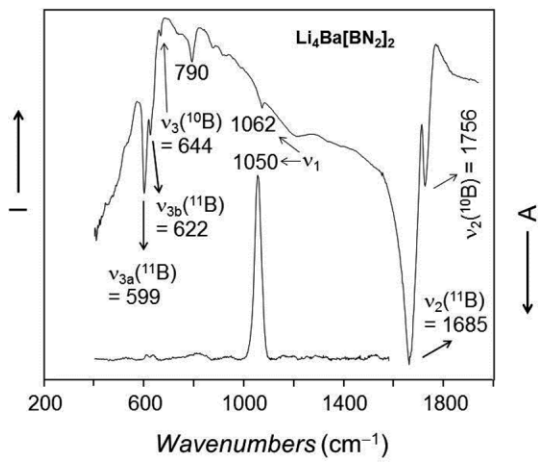


Figure 5. IR and Raman vibrational spectra of $Li_4Ba[BN_2]_2$ with intensity I (Raman) and absorption A (IR) in arbitrary units. Wavenumbers of the fundamentals are given along with the corresponding modes.

Using the equations for vibrational motion of a linear triatomic molecule[42], one obtains for the (B–N) valence, interaction and deformation force constants f, f' and f_D in N·cm^{-1}: 7.81, 1.28, and 0.43. A comparison of the (B–N) valence frequencies and force constants of the title compound

 © 2017 WILEY-VCH Verlag GmbH & Co. KGaA, Weinheim

with those of the related nitridoborates such as $Li_3[BN_2]$, $Ba_3[BN_2]_2$, and $LiBa_4[BN_2]_2$ reveals a close resemblance to the pure lithium compound [$Li_3[BN_2]$: ν_1 = 1057 cm^{-1}, f = 7.87 N·cm^{-1}]. The values for the Ba compounds are significantly lower: $Ba_3[BN_2]_2$: ν_1 = 1028 cm^{-1}, f = 7.54 N·cm^{-1} and $LiBa_4[BN_2]_3$: ν_1 = 1022 cm^{-1}, f = 7.34 N·cm^{-1}. The mentioned shifts for the (B–N) frequencies and force constants are directly related to a partial negative charge, which is a qualitative measure for the electron transfer to the [BN_2] group. With growing electronegativity difference (between the metal and N), the electron transfer and likewise the (N–N) repulsion within the anion increases, too. The result is a general decrease of the corresponding force constants and valence frequencies. Regarding that Li is more electronegative than Ba, the trend for the vibrational data of $Li_4Ba[BN_2]_2$ fits quite well in the series with $Li_3[BN_2]$ →$LiBa_4[BN_2]_2$ → $Ba_3[BN_2]_2$ and harmonizes also with that of the previously reported ternary and quaternary nitridoborates and nitridoborate halides[20,22,26,30].

Acknowledgements

The authors would like to thank Koç University Surface Science and Technology Center (KUYTAM) for conducting the Raman and IR measurements.

Keywords: Nitridoborate; Crystal structure; Vibrational spectroscopy; Lithium; Boron

References

[1] B. Blaschkowski, H. Jing, H.-J. Meyer, *Angew. Chem. Int. Ed.* **2002**, *41*, 3322.
[2] J. Goubeau, W. Anselment, *Z. Anorg. Allg. Chem.* **1961**, *310*, 248.
[3] H. Yamane, S. Kikkawa, H. Horiuchi, M. Koizumi, *J. Solid State Chem.* **1986**, *65*, 6.
[4] H. Yamane, S. Kikkawa, M. Koizumi, *J. Solid State Chem.* **1987**, *71*, 1.
[5] F. E. Pinkerton, J. F. Herbst, *J. Appl. Phys.* **2006**, *99*, 113523.
[6] J. Evers, M. Münsterkötter, G. Oehlinger, K. Polborn, B. Sendlinger, *J. Less-Common Met.* **1990**, *162*, L17.
[7] C. Koz, S. Acar, Y. Prots, P. Höhn, M. Somer, *Z. Anorg. Allg. Chem.* **2014**, *640*, 279.
[8] H. Womelsdorf, H.-J. Meyer, *Z. Anorg. Allg. Chem.* **1994**, *620*, 262.
[9] O. Reckeweg, F. J. DiSalvo, M. Somer, *J. Alloys Compd.* **2003**, *361*, 102.
[10] M. Somer, C. Gül, R. Müllmann, B. D. Mosel, R. K. Kremer, R. Pöttgen, *Z. Anorg. Allg. Chem.* **2004**, *630*, 389.
[11] M. Häberlen, J. Glaser, H.-J. Meyer, *J. Solid State Chem.* **2005**, *178*, 1478.
[12] M. Häberlen, *Synthese, Kristallstrukturen und Phasenübergänge der Nitridoborate der Erdalkalimetalle*, Dissertation, Universität Tübingen, Germany, **2006**.
[13] U. Herterich, J. Curda, K. Peters, M. Somer, H. G. von Schnering, *Z. Kristallogr.* **1994**, *209*, 617.
[14] M. Somer, U. Herterich, J. Curda, K. Peters, H. G. von Schnering, *Z. Kristallogr.* **1994**, *209*, 182.
[15] S. Seidel, T. Dierkes, T. Jüstel, C. Benndorf, H. Eckert, R. Pöttgen, *Dalton Trans.* **2016**, *45*, 12078.
[16] M. Häberlen, J. Glaser, H.-J. Meyer, *Z. Anorg. Allg. Chem.* **2002**, *628*, 1959.
[17] J. Curda, U. Herterich, K. Peters, M. Somer, H. G. von Schnering, *Z. Kristallogr.* **1994**, *209*, 181.
[18] F. E. Rohrer, *Nitridoborate und Nitridoborat-Halogenide von Erdalkali- und Seltenerdmetallen*, Dissertation 12468, ETH Zürich, Switzerland, **1997**.
[19] F. E. Rohrer, R. Nesper, *J. Solid State Chem.* **1998**, *135*, 194.
[20] I. Kokal, U. Aydemir, Yu. Prots, W. Schnelle, L. Akselrud, P. Höhn, M. Somer, *Z. Kristallogr.* **2011**, *226*, 633.
[21] F. E. Rohrer, R. Nesper, *J. Solid State Chem.* **1999**, *142*, 187.
[22] T. E. Toros, M. Yahyaoglu, U. Aydemir, C. Drahten, L. Akselrud, Yu. Prots, P. Höhn, M. Somer, *Z. Anorg. Allg. Chem.* **2015**, *641*, 2014.
[23] F. E. Rohrer, R. Nesper, *J. Solid State Chem.* **1999**, *142*, 192.
[24] M. Somer, Ö. Yaren, O. Reckweg, Yu. Prots, W. Carillo-Cabrera, *Z. Anorg. Allg. Chem.* **2004**, *630*, 1068.
[25] P. Villars, K. Cenzual, *Pearson's Crystal Data: Crystal Structure Database for Inorganic Compounds* (release 2016/17), ASM International®, Materials Park, Ohio (USA) **2016**.
[26] M. Somer, *Z. Naturforsch. B* **1991**, *46*, 1664.
[27] J. Schölch, T. Dierkes, D. Enseling, M. Ströbele, T. Jüstel, H.-J. Meyer, *Z. Anorg. Allg. Chem.* **2015**, *641*, 803.
[28] M. Ströbele, K. Dolabdjian, D. Enseling, D. Dutczak, B. Mihailova, T. Jüstel, H.-J. Meyer, *Eur. J. Inorg. Chem.* **2015**, 1716.
[29] D. Dutczak, K. M. Wurst, M. Ströbele, D. Enseling, T. Jüstel, H.-J. Meyer, *Eur. J. Inorg. Chem.* **2016**, 861.
[30] M. Somer, U. Herterich, J. Čurda, W. Carillo-Cabrera, A. Zürn, K. Peters, H. G. von Schnering, *Z. Anorg. Allg. Chem.* **2000**, *626*, 625.
[31] K. Yvon, W. Jeitschko, E. Parthé, *J. Appl. Crystallogr.* **1977**, *10*, 73.
[32] L. Palatinus, G. Chapuis, *J. Appl. Crystallogr.* **2007**, *40*, 786.
[33] V. Petříček, M. Dušek, L. Palatinus, *Z. Kristallogr.* **2014**, *229*, 345.
[34] R. Pöttgen, O. Reckeweg, *Z. Kristallogr.* **2017**, *232*, in press, DOI:10.1515/zkri-2017-2043.
[35] L. Unverfehrt, M. Ströbele, J. Glaser, H.-J. Meyer, *Z. Anorg. Allg. Chem.* **2009**, *635*, 1947.
[36] M. G. Down, M. J. Haley, P. Hubberstey, R. J. Pulham, A. E. Thunder, *J. Chem. Soc., Chem. Commun.* **1978**, 52.
[37] I. D. Brown, *Chem. Soc. Rev.* **1978**, *7*, 359.
[38] R. Hoppe, S. Voigt, H. Glaum, J. Kissel, H. P. Müller, K. Bernet, *J. Less-Common Met.* **1989**, *156*, 105.
[39] M. Nespolo, B. Guillot, *J. Appl. Crystallogr.* **2016**, *49*, 317.
[40] I. D. Brown, D. Altermatt, *Acta Crystallogr., Sect. B* **1985**, *41*, 244.
[41] N. E. Brese, M. O'Keeffe, *Acta Crystallogr., Sect. B* **1991**, *47*, 192.
[42] H. Siebert, *Anwendungen der Schwingungsspektroskopie in der Anorganischen Chemie*, Springer, Berlin Heidelberg, **1966**.

Received: February 20, 2017
Published Online: April 7, 2017

 © 2017 WILEY-VCH Verlag GmbH & Co. KGaA, Weinheim